

# Superfluidity in Neutron Star Matter

U. Lombardo<sup>1</sup> and H.-J. Schulze<sup>2</sup>

<sup>1</sup> Dipartimento di Fisica, Università di Catania,  
Corso Italia 57, I-95129 Catania, Italy

<sup>2</sup> Departament d'Estructura i Constituents de la Matèria, Universitat de Barcelona,  
Av. Diagonal 647, E-08028 Barcelona, Spain

## 1 Introduction, General Formalism

The research on the superfluidity of neutron matter can be traced back to Migdal's observation that neutron stars are good candidates for being macroscopic superfluid systems [1]. And, in fact, during more than two decades of neutron-star physics the presence of neutron and proton superfluid phases has been invoked to explain the dynamical and thermal evolution of a neutron star. The most striking evidence is given by post-glitch timing observations [2,3], but also the cooling history is strongly influenced by the possible presence of superfluid phases [4,5]. On the theoretical side, the onset of superfluidity in neutron matter or in the more general context of nuclear matter was investigated soon after the formulation of the Bardeen, Cooper, and Schrieffer (BCS) theory of superconductivity [6] and the pairing theory in atomic nuclei [7,8].

The peculiar feature of a nucleon system is that it is a strongly interacting Fermi system with a force which has a short-range repulsive component and a long-range attractive one. The first question raised by scientists was whether or not the strongly repulsive core might prevent the formation of a superfluid state. But it was indeed shown [9] that the BCS approach, based on the mechanism of Cooper pairs, can be successfully extended to nuclear matter and that superfluid states could in fact exist for a wide class of nucleon–nucleon potentials [10]. The second question is related to the fact that the superfluid state of nuclear matter is a self-sustaining state in the sense that nucleons participating to the pairing coupling also screen the pairing itself. From this point of view one expects the strong correlations to play an important role in delimiting the magnitude of the pairing gap. Therefore it appears necessary to go beyond the pure BCS approach and properly add the effects of the medium polarization as self-energy and vertex corrections.

Since the neutron star “laboratory” can only provide an indirect evidence of the nucleon pairing in infinite matter and its relation with the pairing in nuclei is still too much model dependent, we need to rely on very accurate quantitative theoretical predictions of its properties such as energy gap, superfluidity density domain, critical temperature, and other physical quantities associated with the various superfluid states. These quantities may only be obtained from *ab initio* calculations, i.e., microscopic approaches using as input the bare nucleon-nucleon interaction, because we are exploring a density domain much wider than the saturation region where phenomenological interactions such as Skyrme forces

are well suited. There is a more basic reason to refrain from using effective interactions, that is a double counting of the particle-particle (p-p) correlations incorporated in the effective interaction, but also in the gap equation.

Fortunately, for more than two decades *realistic* potentials, based on field-theoretical approaches, have been supplied to describe the bare nucleon-nucleon interaction. The term ‘realistic’ means that the parameters contained in such potentials are adjusted to simultaneously reproduce the experimental phase shifts of nucleon-nucleon scattering and the binding energies of the lightest nuclei.

In this chapter the problem of superfluidity in neutron matter is surveyed and special emphasis is devoted to new theoretical developments and calculations. In the following section the general formalism of pairing in a strongly interacting Fermi system is presented. In Sect. 2 the possible superfluid states of nucleon matter are described within the BCS theory extended to non-zero angular momentum. In the last section some aspects of the generalized gap equation will be discussed, including the medium polarization effects at very low density (Sect. 3.1), the induced interaction approach (Sect. 3.2), and the role of self-energy corrections (Sect. 3.3).

We mention three previous works for a comprehensive study of superfluidity in nuclear matter: the early papers based on the generalized BCS-Bogolyubov theory [11,12], which already give a systematic survey of most superfluid states of nuclear matter; the second one [13], based on the method of the correlated basis functions, mainly focussed on the  $^1S_0$  pairing, but containing a wide discussion of the important medium correlation effects; and lastly, a recent more general overview of pairing in nuclear matter [14].

### 1.1 Green Function Formalism, Generalized Gap Equation

In this section we briefly review the main points of the treatment of a superfluid Fermi system within the Green function formalism. A detailed account is given in various textbooks [15,16,17,18,19,20].

The principal equations describing a superfluid system are the Gorkov equations, that can be considered a generalization of the Dyson equation for a normal Fermi system. A diagrammatic representation of the Gorkov equations is shown in Fig. 1(a). They express the relation between normal and anomalous propagators  $G$  and  $F$ , defined by

$$G(1, 2) = \frac{1}{i} \langle T(\Psi_1 \Psi_2^\dagger) \rangle, \quad (1a)$$

$$F(1, 2) = \frac{1}{i} \langle T(\Psi_1 \Psi_2) \rangle, \quad (1b)$$

and the self-energy  $\Sigma$  and gap function  $\Delta$ . In a homogeneous system, these four quantities depend only on a four-vector  $k = (k_0, \mathbf{k})$  and can be written as  $2 \times 2$  matrices in spin space, for example,

$$\Delta(k) = \begin{pmatrix} \Delta_{\uparrow\uparrow} & \Delta_{\uparrow\downarrow} \\ \Delta_{\downarrow\uparrow} & \Delta_{\downarrow\downarrow} \end{pmatrix} (k). \quad (2)$$

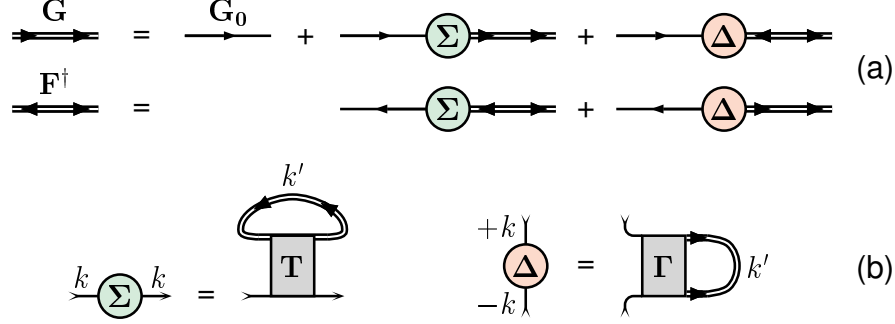


**Fig. 1.** (a) Diagrammatic representation of the Gorkov equations. (b) Equations for the self-energy  $\Sigma$  and gap function  $\Delta$

Using the free fermion propagator

$$G_0(k) = \frac{e^{i0k_0}}{k_0 - \mathbf{k}^2/2m + \mu + i0k_0}, \quad (3)$$

and defining

$$\varepsilon(k) = \frac{\mathbf{k}^2}{2m} + \Sigma(k_0, \mathbf{k}) - \mu, \quad (4)$$

one can write the system of equations explicitly as

$$\begin{pmatrix} [k_0 - \varepsilon(+k)]\mathbf{1} & \Delta(k) \\ \Delta^\dagger(k) & [k_0 + \varepsilon(-k)]\mathbf{1} \end{pmatrix} \begin{pmatrix} \mathbf{G}(k) \\ \mathbf{F}^\dagger(k) \end{pmatrix} = \begin{pmatrix} \mathbf{1} \\ \mathbf{0} \end{pmatrix}, \quad (5)$$

where  $\mathbf{1}$  denotes the two-dimensional unit matrix. In order to take into account at the same time pairing correlations  $\Delta_S$  with spin  $S = 0$  and  $S = 1$ , one can make the ansatz

$$\Delta = \begin{pmatrix} 0 & +\Delta_0 + i\Delta_1 \\ -\Delta_0 + i\Delta_1 & 0 \end{pmatrix}, \quad (6)$$

and equivalently for  $\mathbf{F}^\dagger$ , whereas the self-energy  $\Sigma$  and  $\mathbf{G}$  are diagonal in the spin indices. If the ground state is assumed to be time-reversal invariant, the gap function has in general the structure of a unitary triplet state [21,22], i.e., it fulfills

$$\Delta^\dagger(k)\Delta(k) = \Delta(k)^2\mathbf{1}, \quad (7)$$

where by  $\Delta(k)^2$  we denote the determinant of  $\Delta$  in spin space.

The system Eq. (5) can then be inverted with the solution

$$G(k) = \frac{k_0 + \varepsilon(-k)}{D(k)}, \quad (8a)$$

$$F_S^\dagger(k) = \frac{\Delta_S(k)}{D(k)}, \quad (8b)$$

where

$$D(k) = [k_0 - \varepsilon(+k)] [k_0 + \varepsilon(-k)] - \Delta_0(k)^2 - \Delta_1(k)^2, \quad (9)$$

that expresses the propagators  $G$  and  $F^\dagger$  in terms of  $\Sigma$  and  $\Delta$ , respectively.

In order to determine uniquely the four quantities one needs two more equations, which relate  $\Sigma$  and  $\Delta$  to the interaction. These equations are displayed in Fig. 1(b) and read explicitly

$$\Sigma_{\alpha\alpha}(k) = \frac{1}{i} \int \frac{d^4 k'}{(2\pi)^4} \sum_{\beta} \langle k\alpha, k'\beta | T | k\alpha, k'\beta \rangle G_{\beta\beta}(k'), \quad (10a)$$

$$\Delta_{\alpha\beta}(k) = i \int \frac{d^4 k'}{(2\pi)^4} \sum_{\alpha', \beta'} \langle k\alpha, -k\beta | \Gamma | k'\alpha', -k'\beta' \rangle F_{\alpha'\beta'}(k'), \quad (10b)$$

where greek letters denote spin indices and  $T$  and  $\Gamma$  are the scattering matrix and the irreducible interaction kernel, respectively. Clearly these equations cannot be solved in full generality, but one has to recur to some approximation at this stage. The simplest, very common, BCS approximation, is to replace  $T$  and  $\Gamma$  by the leading term, namely the bare interaction  $V$ . In this case the interaction is energy independent and the  $k_0$  integration in Eqs. (10a,10b) can be carried out trivially, leading to

$$\Sigma(\mathbf{k}) = \sum_{\mathbf{k}'} \frac{v_{\mathbf{k}'}}{2} \left[ \langle \mathbf{k}, \mathbf{k}' | V_0 + 3V_1 | \mathbf{k}, \mathbf{k}' \rangle - \langle \mathbf{k}, \mathbf{k}' | 3V_1 - V_0 | \mathbf{k}', \mathbf{k} \rangle \right], \quad v^2 = \frac{1}{2} \left( 1 - \frac{\varepsilon}{E} \right), \quad (11a)$$

$$\Delta_S(\mathbf{k}) = \sum_{\mathbf{k}'} (u_S v)_{\mathbf{k}'} \langle \mathbf{k}', -\mathbf{k}' | V_S | +\mathbf{k}, -\mathbf{k} \rangle_a, \quad u_S v = \frac{-\Delta_S}{2E}, \quad (11b)$$

where

$$E^2 = \varepsilon^2 + \Delta_0^2 + \Delta_1^2, \quad \varepsilon = \frac{\mathbf{k}^2}{2m} + \Sigma(\mathbf{k}) - \mu. \quad (12)$$

Together with an equation fixing the chemical potential  $\mu$  for given density  $\rho$ ,

$$\rho = 2 \sum_{\mathbf{k}} v_{\mathbf{k}}^2, \quad (13)$$

this is the coupled set of equations that needs to be solved in order to find the Hartree-Fock self-energy  $\Sigma_{\text{HF}}(\mathbf{k})$  and the BCS gap function  $\Delta_{\text{BCS}}(\mathbf{k})$  in a superfluid system. In contrast to a normal Fermi system, the smooth occupation numbers  $v_{\mathbf{k}}^2$  instead of the Fermi function  $\theta(k_F - |\mathbf{k}|)$  appear in the HF equation.

## 2 BCS Approximation

In this section we present the solutions of the BCS gap equation

$$\Delta_{TS}(\mathbf{k}) = - \sum_{\mathbf{k}'} \langle \mathbf{k} | V_{TS} | \mathbf{k}' \rangle \frac{\Delta_{TS}(\mathbf{k}')}{2E(\mathbf{k}')}, \quad (14a)$$

$$\rho = \frac{k_F^3}{3\pi^2} = 2 \sum_{\mathbf{k}} \frac{1}{2} \left[ 1 - \frac{\varepsilon(\mathbf{k})}{E(\mathbf{k})} \right], \quad (14b)$$

where

$$E(\mathbf{k})^2 = \epsilon(\mathbf{k})^2 + \sum_{T,S=0,1} \Delta_{TS}(\mathbf{k})^2, \quad \epsilon(\mathbf{k}) = e(\mathbf{k}) - \mu \quad (15)$$

with  $\mu$  being the chemical potential and  $e(\mathbf{k})$  the single-particle spectrum. Different realistic nucleon-nucleon potentials  $V$  [23,24,25,26,27,28] will be used as input. The equations are valid for pure neutron matter ( $T = 1$ ) and also for *symmetric* nuclear matter ( $T = 0, 1$ ), having extended the derivation in the previous section by including the isospin quantum number  $T$  in analogy to the spin  $S$ .

## 2.1 Pairing in Different Partial Waves

In order to reduce the three-dimensional integral equation (14a) to a set of one-dimensional ones, it is advantageous to perform partial wave expansions of the potential and the gap function. In this way one arrives at separate equations in the different ( $TSSL'$ ) channels of the interaction, provided an angle-average approximation is made by replacing  $\Delta(\mathbf{k})^2 \rightarrow \int d\hat{\mathbf{k}}/4\pi \Delta(\mathbf{k})^2$  in Eq. (15). The following equations for the partial wave components of the gap function are then obtained [12,29,30,31,32,33]:

$$\Delta_{TSL}(k) = -\frac{1}{\pi} \int_0^\infty dk' k'^2 \sum_{L'} \frac{V_{LL'}^{TS}(k, k')}{\sqrt{\epsilon(k')^2 + \Delta(k')^2}} \Delta_{TSL'}(k'), \quad (16)$$

where

$$\Delta(k)^2 = \sum_{T,S,L} \Delta_{TSL}(k)^2, \quad (17)$$

and with the matrix elements of the bare potential in momentum space

$$V_{LL'}^{TS}(k, k') = \int_0^\infty dr r^2 j_{L'}(k'r) V_{LL'}^{TS}(r) j_L(kr). \quad (18)$$

It should be noted that the different equations are still coupled due to the fact that the total gap appearing in the denominator on the r.h.s. of Eq. (16) is the r.m.s. value of the gaps in the different partial waves. The gap equation allows in principle the coexistence of pairing correlations with different quantum numbers ( $TS$ ), even though the different ( $TS$ ) channels are not mixed by the interaction. In practice, however, so far no such mixed solutions of the gap equation have been found: even if at a given density two or more uncoupled solutions exist, the strong nonlinear character of the gap equation prohibits a coupled solution. (In finite nuclei such mixed solutions seem to exist under certain conditions [34]). This means that in practice this ( $TS$ )-coupling can be neglected and that at a given density the solution of the uncoupled gap equation with the largest gap is the energetically favoured one.

The only case when it is clearly necessary to keep the coupled equations is the mixing of partial waves due to the tensor potential. In this case the gap

equation can be written in matrix form (for given  $S = 1, T, L$ ):

$$\begin{pmatrix} \Delta_L \\ \Delta_{L+2} \end{pmatrix}(k) = -\frac{1}{\pi} \int_0^\infty dk' k'^2 \frac{1}{E(k')} \begin{pmatrix} V_{L,L} & V_{L,L+2} \\ V_{L+2,L} & V_{L+2,L+2} \end{pmatrix}(k, k') \begin{pmatrix} \Delta_L \\ \Delta_{L+2} \end{pmatrix}(k') \quad (19)$$

with

$$E(k)^2 = [e(k) - \mu]^2 + \Delta_L(k)^2 + \Delta_{L+2}(k)^2. \quad (20)$$

This is relevant equation for the  ${}^3SD_1$  ( $T = 0$ ) and  ${}^3PF_2$  ( $T = 1$ ) channels, for example.

Let us finally mention that usually, apart from the  ${}^3SD_1$  channel, the two equations (14a) and (14b) can be decoupled by setting  $\mu = e(k_F)$ . The reason is the small value of the ratio  $\Delta/\mu$ , so that a Fermi surface is still quite well defined.

We come now to the presentation of the results that are obtained by solving the previous equations numerically, using a kinetic energy spectrum  $e(k) = k^2/2m$  for the moment. In practice, one finds in pure neutron matter ( $T = 1$ ) gaps only in the  ${}^1S_0$  [12,13,35,36,37,38] and  ${}^3PF_2$  [12,29,30,31,32,33] partial waves. They are reported in Figs. 2 and 3, respectively. It can be observed that the maximum pairing gap is about 3 MeV in the  ${}^1S_0$  channel and of the order of 1 MeV in the  ${}^3PF_2$  wave. It is remarkable that solutions obtained with different nucleon-nucleon potentials are nearly indistinguishable in the  ${}^1S_0$  case, whereas in the  ${}^3PF_2$  wave such good agreement can only be observed up to  $k_F \approx 2 \text{ fm}^{-1}$  (with the exception of the Argonne  $V_{14}$  potential that is not very well fitted

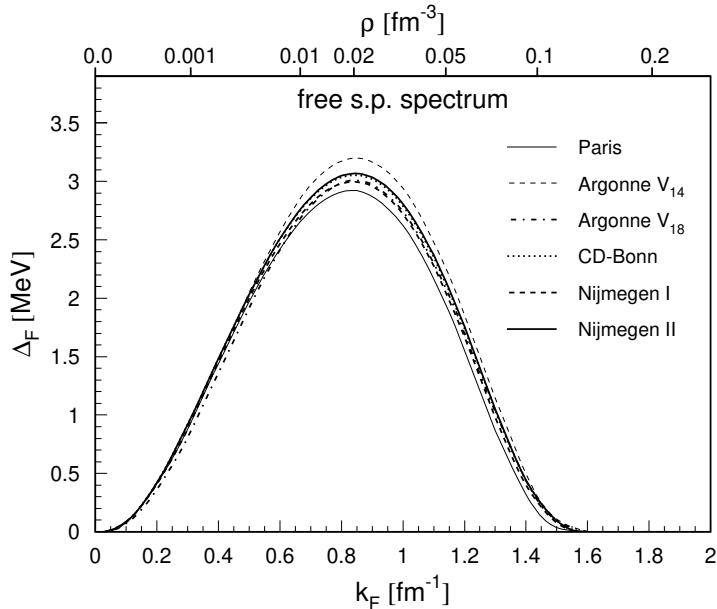


**Fig. 2.**  ${}^1S_0$  gap evaluated in BCS approximation with free single-particle spectrum and different potentials

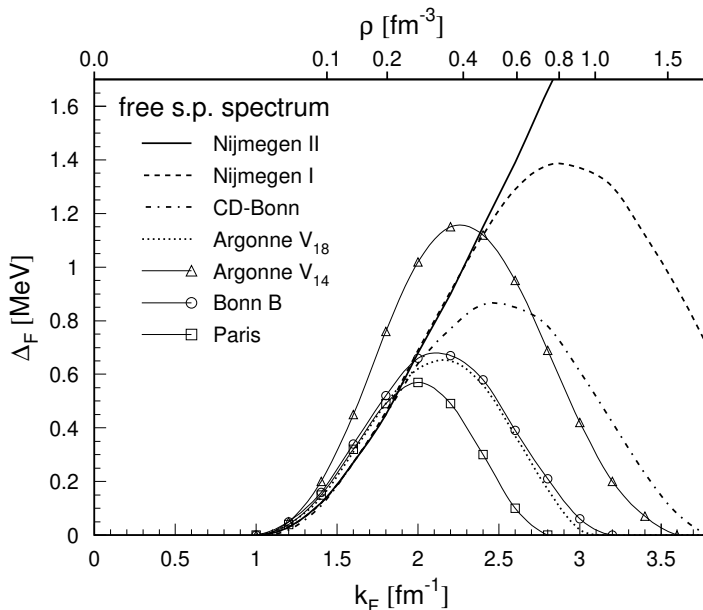


**Fig. 3.**  ${}^3PF_2$  gap evaluated in BCS approximation with free single-particle spectrum and different potentials

to the phase shifts), from where on the predictions start to diverge from each other. The reason [32,38] is the fact that the various potentials are constrained by the phase shifts only up to scattering energies  $E_{\text{lab}}$  of about 350 MeV, which roughly corresponds to a Fermi momentum of  $k_F \approx \sqrt{mE_{\text{lab}}/2} \approx 2 \text{ fm}^{-1}$ . Thus even on the BCS level the gap in the  ${}^3PF_2$  channel at a neutron density higher than  $\approx 0.3 \text{ fm}^{-3}$  is at the moment not known. Apart from that it is clear that the BCS approximation is not reliable at the very large densities for which a gap is predicted in Fig. 3. However, nobody has so far attempted to include polarization effects in this channel.

Let us mention here for completeness that in symmetric nuclear matter one finds very strong pairing of the order of 10 MeV in the  ${}^3SD_1(T=0)$  channel, reminiscent of the deuteron bound state [12,21,22,39,40,41,42,43,44,45,46], and also a gap of the order of 1 MeV in the  ${}^3D_2$  wave [12,47]. This, however, is probably not very relevant for neutron star physics, since a prerequisite for this  $T=0$  neutron-proton pairing to take place is the existence of (nearly) isospin symmetric nuclear matter, the pairing correlations being rapidly destroyed by increasing asymmetry [48,49,50]. We will therefore not discuss this type of pairing further on.

## 2.2 Pairing Gaps in Neutron Star Matter

Let us now come to the  $T=1$  gaps that can be expected in isospin asymmetric (beta-stable and charge neutral) neutron star matter. On the BCS level, the only

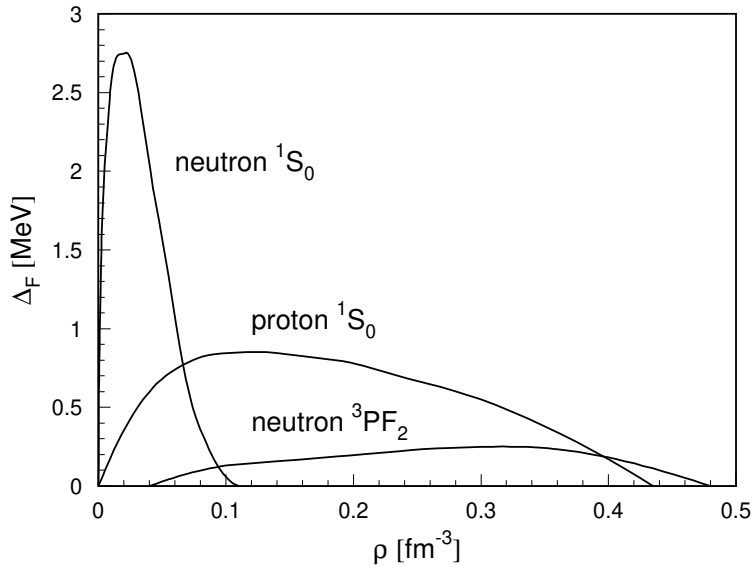


**Fig. 4.** The different  $T = 1$  gaps in neutron star matter as a function of total nucleonic density

influence of isospin asymmetry on these gaps is via the neutron single-particle energy  $e(k)$  appearing in the gap equation. Calculations have been performed using  $e(k)$  determined in the BHF approximation extended to asymmetric nuclear matter [30,31,51,52,53,54,55,56], and typical results are shown in Fig. 4. One observes that  $^1S_0$  pairing can take place independently in the neutron and in the proton component of the matter. If plotted as a function of total baryon density, the neutron pairing occurs naturally at lower density and with a larger amplitude than the proton pairing, because at the higher density the proton effective mass is smaller and the pairing therefore more reduced. The same is true for the  $^3PF_2$  pairing in the neutron component, which is strongly reduced with respect to the calculation with a free spectrum shown in Fig. 3 above. We stress that the results displayed in Fig. 4 can only be qualitative, because they clearly depend on the details (in particular the proton fraction) of the equation of state that is used. The results shown were obtained with a BHF EOS based on the Argonne  $V_{14}$  potential and involving  $n$ ,  $p$ ,  $e$ ,  $\mu$  components [52].

### 3 Beyond BCS

In the previous section we have presented many results that were all obtained within the BCS approximation. However, as has been explained in the introduction, this approximation amounts to a mean-field approach, equivalent to and consistent with the Hartree-Fock approximation in a normal Fermi system. More precisely, the BCS approximation neglects completely any contribution



beyond the bare potential to the interaction kernel  $\Gamma$  appearing in the general gap equation (10b).

Going consistently beyond the BCS approximation is however a very difficult task and has been only partially achieved so far. We will review in the following sections some aspects of these extensions. We begin with a discussion of the situation at extremely low density, where certain analytical results are known. Following that, the general framework at more relevant densities will be set up, and we will briefly present the results that have been obtained so far by various authors. Finally, in the last section, we will focus on a certain part of the problem that has recently been tackled, namely the treatment of the energy dependence of the self-energy that appears in the gap equation.

### 3.1 Low Density

In order to derive an exact analytical result for the pairing gap including polarization effects that is valid at very low density (more precisely, for  $k_F \ll 1/|a|$ , where  $a$  is the relevant scattering length), we begin again with the BCS gap equation,

$$\Delta_k = - \sum_{k'} V_{kk'} \frac{1}{2E_{k'}} \Delta_{k'} , \quad E_k = \sqrt{(e_k - e_F)^2 + \Delta_k^2} . \quad (21)$$

It is then useful [36,54,57] to introduce a modified interaction  $T$  that is given by the solution of the integral equation

$$T_{kk'} = V_{kk'} - \sum_{k''} T_{kk''} F_{k''} V_{k''k'} , \quad (22)$$

where  $F_k$  is for the moment an arbitrary function. (We have used the symbol  $T$ , although in general this quantity is not to be identified with the scattering matrix). Making use of this equation, the gap equation is transformed into

$$\Delta_k = - \sum_{k'} T_{kk'} \left( \frac{1}{2E_{k'}} - F_{k'} \right) \Delta_{k'} . \quad (23)$$

Of particular interest is now the choice  $F_k = \text{sgn}(k - k_F)/2E_k$ , which leads to the set of equations

$$\Delta_k = -2 \sum_{k' < k_F} T_{kk'} \frac{1}{2E_{k'}} \Delta_{k'} , \quad (24)$$

$$T_{kk'} = V_{kk'} - \sum_{k''} T_{kk''} \frac{\text{sgn}(k'' - k_F)}{2E_{k''}} V_{k''k'} . \quad (25)$$

Therefore, in the limit  $\Delta/e_F \rightarrow 0$  that is approached with vanishing density,  $T$  does become identical to the free scattering matrix, because  $E_k \rightarrow |e_k - e_F|$  in this situation. At the same time, in the gap equation (24) the interaction  $T$

is now cut off at  $k' = k_F$  (at the cost of introducing a factor 2), so that with vanishing density it is ultimately sufficient to use the low-energy result [58] for the  $T$ -matrix:

$$T_{kk'} \rightarrow T_{00} = \frac{4\pi a_{nn}}{m}, \quad (26)$$

where  $a_{nn} = -18.8$  fm is the neutron-neutron scattering length. This yields finally the gap equation

$$1 = -\frac{4k_F a_{nn}}{\pi} \int_0^1 dx \frac{x^2}{\sqrt{(1-x^2)^2 + (\Delta/e_F)^2}}, \quad (27)$$

which in the limit  $\Delta/e_F \rightarrow 0$  is solved by [37,59,60,61]

$$\Delta(k_F) \xrightarrow{k_F \rightarrow 0} \Delta_0(k_F) = \frac{8}{e^2} \frac{k_F^2}{2m} \exp\left[\frac{\pi}{2k_F a_{nn}}\right]. \quad (28)$$

This is the universal asymptotic result for the BCS pairing gap in a low-density Fermi system with negative scattering length. Unfortunately its validity is limited to the region  $k_F \ll 1/|a_{nn}| \approx 0.05$  fm<sup>-1</sup>, far below the densities of interest for neutron star physics or even pairing in finite nuclei.

Going now beyond the BCS approximation, in the low-density limit one should take into account the corrections to the interaction kernel that are of leading order in density. Diagrammatically these are the polarization diagrams of first order (i.e., comprising one polarization ‘‘bubble’’) that are displayed in Fig. 5. The interaction appearing in these diagrams is in the present case the free scattering matrix  $T$ . It can be shown [59] that in the low-density limit it is again sufficient to neglect the momentum dependence of the  $T$ -matrix, as in Eq. (26). One obtains then for the lowest-order polarization interaction

$$W_{1S_0}(k, k') = -\frac{T_{00}^2}{8\pi} \frac{1}{2kk'} \int_{|k-k'|}^{k+k'} dq q \Pi(q), \quad (29)$$

where

$$\Pi(q) = -\frac{mk_F}{\pi^2} \left[ \frac{1}{2} + \frac{1-x^2}{4x} \ln \left| \frac{1+x}{1-x} \right| \right], \quad x = \frac{q}{2k_F} \quad (30)$$

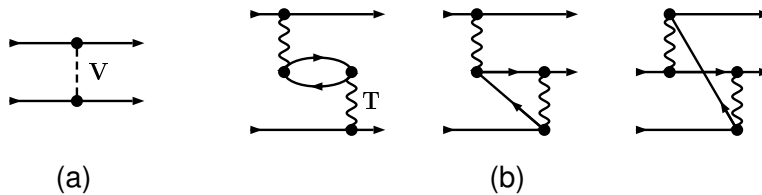


**Fig. 5.** (a) Bare potential and (b) first-order (direct and exchange) polarization diagrams contributing to the interaction kernel in the low-density limit

is the static Lindhard function [58]. Thus the lowest-order polarization modifies the BCS interaction kernel Eq. (18) by a (repulsive) term proportional to  $k_F$ , whereas any other polarization diagram contributes only in higher order of  $k_F$ .

We can use this result and insert it into the previously obtained approximation in the BCS case:

$$\Delta(k_F) \xrightarrow{k_F \rightarrow 0} \frac{8}{e^2} \frac{k_F^2}{2m} \exp\left[\frac{\pi/2}{\kappa + c\kappa^2}\right], \quad \kappa = k_F a_{nn}, \quad (31)$$

where

$$c = -\frac{2\pi}{mk_F} \int_0^{2k_F} \frac{dq q}{2k_F^2} \Pi(q) = \frac{2}{3\pi} (1 + 2 \ln 2) \approx 0.506 \quad (32)$$

accounts for the polarization effects to first order. Expanding now the argument of the exponential up to second order in  $\kappa$ , one obtains for the ratio relative to the BCS value, Eq. (28),

$$\frac{\Delta(k_F)}{\Delta_0(k_F)} = \exp\left[-\frac{\pi}{2}c [1 - c\kappa + \mathcal{O}(\kappa^2)]\right] \quad (33)$$

$$\approx \left[\frac{1}{(4e)^{1/3}}\right]^{(1-c\kappa)} \quad (34)$$

$$\xrightarrow{k_F \rightarrow 0} \frac{1}{(4e)^{1/3}}. \quad (35)$$

Let us stress that the above ‘‘derivation’’ of this result can only be considered heuristic. A rigorous proof was given originally in Ref. [59].

Therefore, one arrives at the striking conclusion that in the low-density limit the polarization corrections suppress the BCS gap by a factor  $(4e)^{-1/3} \approx 0.45$ , independent of the strength of the interaction  $a_{nn}$ . This is quite surprising, since the polarization interaction clearly vanishes with vanishing density; its effect on the pairing gap, however, does not. The reason is the nonanalytical dependence of the gap on the interaction strength, as expressed by Eq. (28).

All this means that the BCS approximation cannot even be trusted at very low density, and that one can in general expect quite strong modifications due to polarization effects at higher density as well.

This low-density behaviour of neutron pairing could be met in the study of exotic nuclei with a long density tail or in nuclei embedded in a neutron matter environment, as occurring in the neutron star crust.

### 3.2 General Polarization Effects

To go beyond the simple low-density approximations derived before requires considerable effort and has in fact so far not been accomplished in a satisfactory manner, so that ultimate results cannot be presented here. The reason is that many effects that could be neglected in the low-density limit become important

now, and that on the other hand the pairing gap is extremely sensitive to even slight changes of the interaction kernel.

First, outside the low-density region  $k_F \ll 1/|a_{nn}|$ , the interaction kernel has to be extended beyond the lowest-order polarization diagrams. This means summing up polarization diagrams of all orders in the particle-particle channel, but also including them in the particle-hole channel, replacing the  $T$ -matrix by the general particle-hole interaction  $F$ . In this way a self-consistent scheme is established that is depicted in Fig. 6. It requires as input the Brueckner  $G$ -matrix

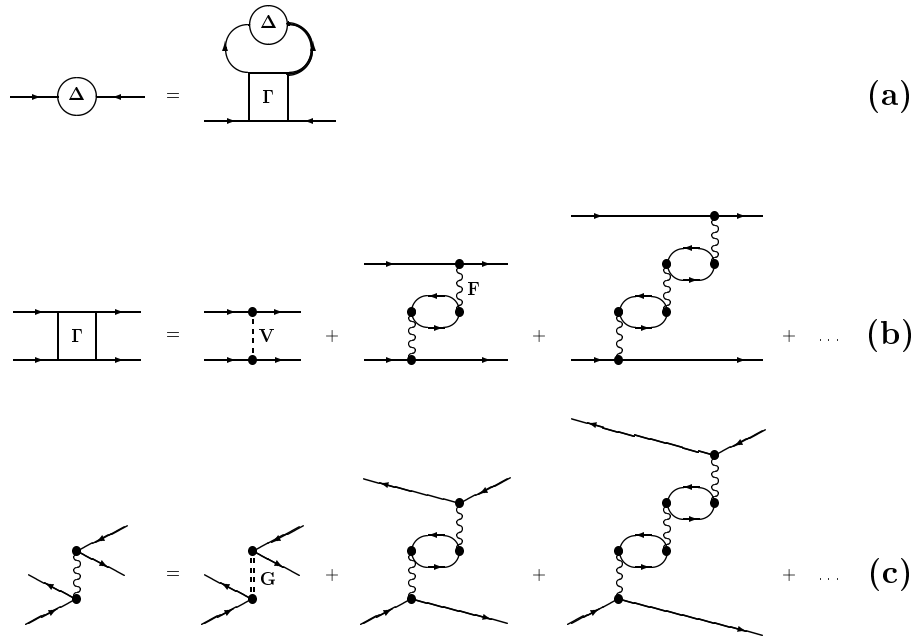


**Fig. 6.** Determination of the interaction kernel  $\Gamma$  in the gap equation (a): Polarization diagrams appear in the particle-particle channel (b) as well as in the particle-hole channel (c). The leading diagrams in these channels are the bare potential  $V$  (dashed line) and the  $G$ -matrix (double-dashed line), respectively

and yields ideally the interactions in the particle-particle as well as particle-hole channel,  $\Gamma$  and  $F$ , respectively. It is clear that in practice an exact solution is impossible, but that usually strong approximations have to be performed that cast a doubt on the reliability of the results that are obtained. We will later discuss this point in some more detail.

Second, related to the previous item, the energy dependence of the full gap equation [see Eq. (10b)] needs to be taken into account. This is obvious, since the interaction kernel becomes now a complex, energy-dependent quantity. To our knowledge, this problem has so far not been studied in detail in the literature. It

is therefore not known how far the gap could be changed by this more elaborate treatment of the equations.

Third, and in connection with the two previous points, the choice of a particular interaction kernel requires also the choice of a compatible self-energy appearing in the gap equation. This will be explained in more detail in the following section, as it has recently been addressed in the literature.

It should be clear by now that the influence of medium effects on pairing constitutes an extremely difficult problem. Consequently the results that can be found in the literature [13,62,63,64,65,66] addressing this task in certain approximations agree only on the fact that generally a strong reduction with respect to the BCS gap is obtained. A collection of these results is displayed in Fig. 7. It can be seen that the precise amount and density dependence of the suppression vary substantially between the different approaches and must be considered unknown for the time being.

The most advanced description of medium polarization effects is based on the Babu-Brown induced interaction model [67,68,69,70,71,72]. The microscopic derivation of the effective interaction starts from the following physical idea: The particle-hole (p-h) interaction can be considered as made of a *direct* component containing the short-range correlations and an *induced* component due to the exchange of the collective excitations of the medium.

Let us consider a homogeneous system of fermions interacting via an instantaneous potential  $V$ , which is also translationally and rotationally invariant. Collective excitations are described by the ring series, which can easily be summed

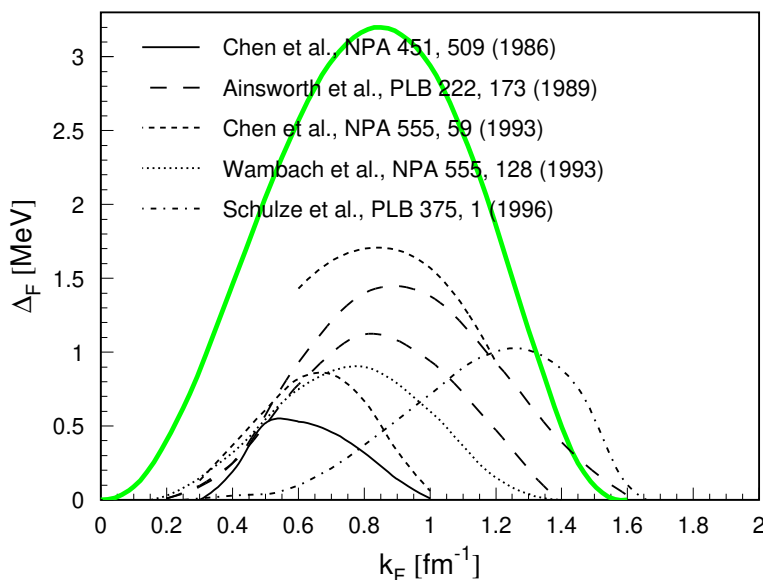


**Fig. 7.** The  $^1S_0$  gap in pure neutron matter predicted in several publications taking account of polarization effects. The curve in the background shows the BCS result

up [58], and the p-h interaction can be written as (disregarding for the moment spin degrees of freedom)

$$V_{\text{ph}}(q) = V(q) + \frac{\Pi(q)V(q)^2}{1 - \Pi(q)V(q)}. \quad (36)$$

In this simple case the interaction itself plays the role of the direct term and the sum of the ring series that of the induced term.

In the nuclear case the presence of the hard core imposes the bare interaction  $V$  to be renormalized in order to incorporate the short-range correlations. This goal is reached by introducing the  $G$ -matrix, which sums particle-particle (p-p) ladder diagrams to all orders, and the diagrammatic expansion can be recast just replacing  $V$  by  $G$ . But now the new ring series cannot be summed up any longer, mainly since the  $G$ -matrix is nonlocal. An averaging procedure has been devised to bring the  $G$ -matrix into a local form  $G(q)$  [66]. Then, in analogy to Eq. (36), the p-h interaction  $F$  is given by

$$F(q) = G(q) + \frac{\Pi(q)G(q)^2}{1 - \Pi(q)G(q)}. \quad (37)$$

In a simplified version of the theory the direct term now coincides with the  $G$ -matrix and the induced term is the approximate sum of the renormalized ring diagrams. In Fig. 6 the direct term is represented by the first diagram on the r.h.s. of the series (c). The next diagrams form the ring (or bubble) series.

But, since the RPA series with the  $G$ -matrix produces a too strong polarizability of nuclear matter, in the Babu-Brown approach it has been proposed to include in the RPA series the full p-h interaction itself, since the particle (hole) coupling vertex with the p-h bubble can indeed be identified with the irreducible p-h interaction. The series (c) of Fig. 6 is, in fact, the final result of such a procedure, where the wiggles represent the effective p-h interaction  $F$  on either side. If we denote by  $F_d$  the direct interaction ( $G$ -matrix in our case) and by  $F_i$  the induced interaction, the effective p-h interaction can be written in the form (at the Landau limit, in which  $\mathbf{p}_1$  and  $\mathbf{p}_2$  are restricted to the Fermi surface)

$$F(\mathbf{p}_1, \mathbf{p}_2) = F_d(\mathbf{p}_1, \mathbf{p}_2) + F_i(\mathbf{p}_1, \mathbf{p}_2; F), \quad (38)$$

where  $F_i$  is, as said before, the RPA series of Fig. 6(c) with the  $G$ -matrix replaced by  $F$  itself. The previous equation clearly entails a self-consistent procedure to determine the interaction  $F(\mathbf{p}_1, \mathbf{p}_2)$ . Referring to [66] for details, one may reduce Eq. (38) to a numerically tractable form

$$F(q) = G(q) + \frac{\Pi(q)F(q)^2}{1 - \Pi(q)F(q)}, \quad (39)$$

which corresponds to replacing the  $G$ -matrix by  $F$  in the induced term.

Once the irreducible p-h interaction  $F$  has been determined, one can construct the irreducible p-p interaction  $\Gamma$  by performing the transformation of the matrix elements of the interaction from the p-h to the p-p channel. However,

this is not enough, since in the p-p channel a set of additional diagrams must be added arising from p-h diagrams which are reducible in that representation. After including these terms, the interaction contains both direct and exchange terms, which guarantees antisymmetry and Landau sum rules and, in addition, it should simultaneously make the nuclear matter Landau parameter  $F_0$  less negative so that the stability condition is satisfied. The first contributions to the p-p interaction are depicted in line (b) of Fig. 6. We stress once more that they describe the influence of the medium polarization on the nucleon-nucleon interaction within the induced interaction model of Babu-Brown.

We discuss now the effects of medium polarization on the superfluidity of neutron stars in the channel  $^1S_0$ . First of all, the irreducible p-p interaction to be used in the pairing problem must not include any ladder sum already included in the gap equation, and therefore the first term in line (b) of Fig. 6 is the bare neutron-neutron interaction  $V$ . The next terms include the irreducible p-h interaction in the vertices of the p-h bubble. If their momentum dependence is neglected, these vertices can be identified with the Landau parameters [69].

In neutron matter the polarization of the medium is due to density fluctuations and spin-density fluctuations given by

$$\delta\rho_{\mathbf{k}} = \delta\rho_{\mathbf{k}\uparrow} + \delta\rho_{\mathbf{k}\downarrow}, \quad (40a)$$

$$\delta\rho_{\mathbf{k}} = \delta\rho_{\mathbf{k}\uparrow} - \delta\rho_{\mathbf{k}\downarrow}, \quad (40b)$$

respectively. Solving the Babu-Brown self-consistent equation, Eq. (39), with the  $G$ -matrix as direct interaction and the renormalized RPA series as induced interaction, one determines the p-h interaction and eventually, after the Landau angle expansion, the lowest-order Landau parameters  $F_0$ , related to the nuclear compression modulus, and  $G_0$ , related to the spin waves. (In the following the interaction will be expressed in terms of these two Landau parameters for simplicity). Then the effective interaction is calculated including the diagrams of Fig. 6(b). The pairing interaction in the  $^1S_0$  channel is then given by

$$\Gamma_{^1S_0} = V_{^1S_0} + \frac{1}{2k_F^2} \int_0^{2k_F} dq q \left[ \frac{F_0^2 \Pi(q)}{1 - F_0 \Pi(q)} - \frac{3G_0^2 \Pi(q)}{1 - G_0 \Pi(q)} \right]. \quad (41)$$

This equation shows that the medium screening effect is determined by the competition between the attractive term induced by density fluctuations and the repulsive term induced by spin-density fluctuations (first and second term in the bracket, respectively).

As depicted in Fig. 8, the effect of the medium polarization is an overall suppression of the gap due to the prevalence of the spin-density fluctuations over the density fluctuations. A similar effect is found in a less crude calculation [66], as shown in Fig. 7, where the peak value is shifted to higher density. Such a suppression is common to all calculations existing in the literature even if, as to its magnitude, the different predictions do not agree with each other, as shown in Fig. 7.

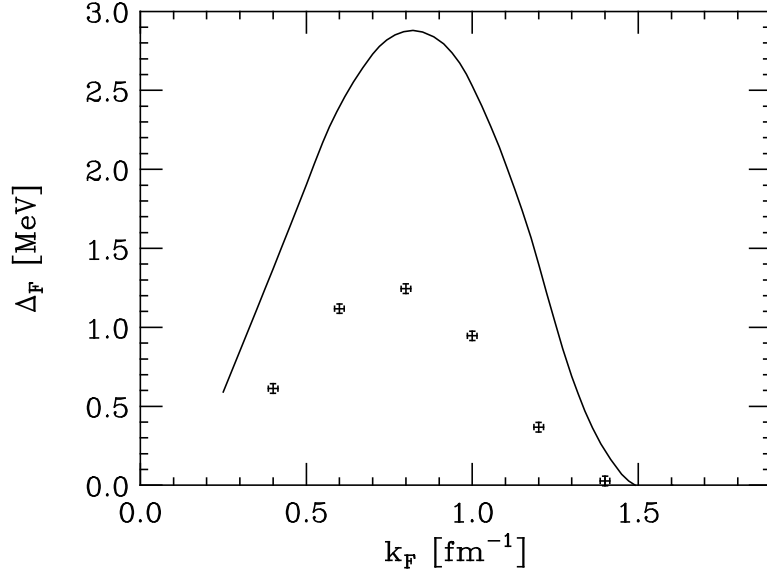


**Fig. 8.**  $^1S_0$  pairing gap in neutron matter as a function of the Fermi momentum  $k_F$ . The full curve corresponds to using the bare  $V_{14}$  potential as direct interaction. The symbols show the effect of the medium polarization described in terms of the Landau parameters, according to Eq. (41)

### 3.3 Self-energy Effects

Dynamical effects of the interaction on the gap function have been completely left aside from the discussion on the medium polarization. So far no solution of the gap equation has been attempted considering the irreducible interaction block as an energy-dependent quantity. On the other hand the energy dependence in the self-energy can affect deeply the magnitude of the energy gap in a strongly correlated Fermi system such as nucleon matter [73,74].

To discuss self-energy effects we come back to the generalized gap equation presented in section 1.1. Let us rewrite Eq. (10b) in the following form (for the  $^1S_0$  channel)

$$\Delta_k(\omega) = - \int \frac{d^3k'}{(2\pi)^3} \int \frac{d\omega'}{2\pi i} \Gamma_{k,k'}(\omega, \omega') \frac{\Delta_{k'}(\omega')}{D_{k'}(\omega')}, \quad (42)$$

with [cf. Eqs. (8a) and (9)]

$$-D_k(\omega) = [G_k(-\omega)G_k^s(\omega)]^{-1} = G_k^{-1}(\omega)G_k^{-1}(-\omega) + \Delta_k^2(\omega). \quad (43)$$

The functions  $G_k(\omega)$  and  $G_k^s(\omega)$  are the nucleon propagators of neutron matter in the normal state and in the superfluid state, respectively. The  $\omega$ -symmetry in the two propagators is to be traced to the time-reversal invariance of the Cooper pairs. The effective interaction  $\Gamma$  is the block of all irreducible diagrams of the



interaction. Since we want to focus only on the self-energy effects, we assume the interaction to be the bare interaction  $V_{k,k'}$ , as in BCS. Then the pairing gap does not depend on the energy (static limit), i.e.,  $\Delta_k(\omega) \equiv \Delta_k$ , and the  $\omega$ -integration can be performed in Eq. (42), once the self-energy has been determined. A general discussion of the analytic  $\omega$ -integration of the gap equation has been given in Ref. [74]. Here we follow a simplified treatment based on the fact that, at each momentum  $k$ , the main contribution to the  $\omega$ -integration comes from the pole of  $G_k(\omega)$ . This latter is the solution of the implicit equation

$$\omega_k = k^2/2m + \Sigma_k(\omega_k) - \mu. \quad (44)$$

Expanding the self-energy around the pole  $\omega_k$  amounts to expanding  $G^{-1}$  itself, which yields

$$G_k^{-1}(\omega) \approx \left(1 - \frac{\partial \Sigma}{\partial \omega} \Big|_{\omega=\omega_k}\right) (\omega - \omega_k), \quad (45)$$

where the prefactor on the r.h.s. is the inverse of the quasiparticle strength  $Z_k$  that will be discussed later. Then the energy dependence of the kernel  $D_k^{-1}(\omega)$  takes the simple form

$$D_k^{-1}(\omega) = \frac{Z_k^2}{\omega^2 - \omega_k^2 - (Z_k \Delta_k)^2}, \quad (46)$$

and the  $\omega$ -integration can be performed in the usual way, leading to

$$\Delta_k = - \int \frac{d^3 k'}{(2\pi)^3} (Z_k V_{k,k'} Z_{k'}) \frac{\Delta_{k'}}{2\sqrt{\omega_{k'}^2 + \Delta_{k'}^2}}. \quad (47)$$

Comparing with the BCS result, Eq. (14a), the new gap equation contains the quasiparticle strength  $Z$  to the second power. Since  $Z$  is significantly less than one in a strongly correlated Fermi system, a substantial suppression of the energy gap is to be expected.

Moreover  $Z$  deviates from unity only in a narrow region around the Fermi surface and hence it is not a severe approximation to restrict the  $\omega$ -integration to only the pole part at the Fermi energy. Expanding then  $\Sigma_k(\omega)$  around the Fermi surface ( $\omega = 0$  and  $k = k_F$ ), Eq. (44) is easily solved and we get  $\omega_k \approx (k^2 - k_F^2)/2m^*$ , where  $m^*$  is the effective mass at  $k_F$  [see Eq. (53)]. The gap equation becomes

$$\Delta_k = -Z_F^2 \int \frac{d^3 k'}{(2\pi)^3} \frac{V_{k,k'} \Delta_{k'}}{2\sqrt{[(k'^2 - k_F^2)/2m^*]^2 + \Delta_{k'}^2}}, \quad (48)$$

where  $Z_F^2$  is the quasiparticle strength at the Fermi surface.

As is well known the pairing modifies the chemical potential which is calculated self-consistently with the gap equation from the closure equation for the average density of neutrons

$$\rho = 2 \int \frac{d^3 k}{(2\pi)^3} \int \frac{d\omega}{2\pi i} G_k^s(\omega^+) \quad (49)$$

$$\approx Z_F \int \frac{d^3 k}{(2\pi)^3} \left[ 1 - \frac{(k^2 - k_F^2)/2m^*}{\sqrt{[(k^2 - k_F^2)/2m^*]^2 + Z_F^2 \Delta_k^2}} \right]. \quad (50)$$

The latter approximation is sufficient to investigate the self-energy effects.

Before we present the predictions based on Eq. (48), we discuss some properties of the self-energy  $\Sigma_k(\omega)$  of neutron matter. In the Brueckner approach [75] the perturbative expansion of  $\Sigma$  can be recast according to the number of hole lines as follows

$$\Sigma_k(\omega) = \Sigma_k^{(1)}(\omega) + \Sigma_k^{(2)}(\omega) + \dots \quad (51)$$

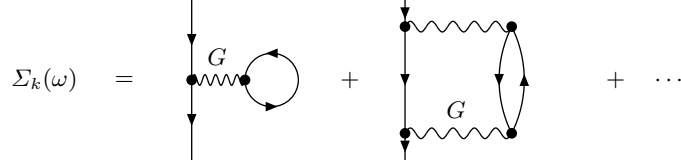


**Fig. 9.** Hole-line expansion of the self-energy

The on-shell values of  $\Sigma^{(1)}$  represent the Brueckner-Hartree-Fock (BHF) mean field (first diagram in Fig. 9); the ones of  $\Sigma^{(2)}$  represent the so-called rearrangement term (second diagram in Fig. 9), which is the largest contribution due to ground-state correlations. The off-shell values of the self-energy are required to solve the generalized gap equation. Fig. 10 displays a typical result for the off-shell neutron self-energy  $\Sigma_k(\omega)$  calculated up to the second order of the hole-line expansion. The calculations are based on Brueckner theory adopting the continuous choice as auxiliary potential [76].

Since we are interested in the behaviour of the self-energy around the Fermi surface ( $k = k_F$  and  $\omega = 0$ ), we may use the expansion

$$\Sigma_k(\omega) \approx \Sigma_{k_F}(0) + \left. \frac{\partial \Sigma}{\partial \omega} \right|_F \omega + \left. \frac{\partial \Sigma}{\partial k} \right|_F (k - k_F). \quad (52)$$

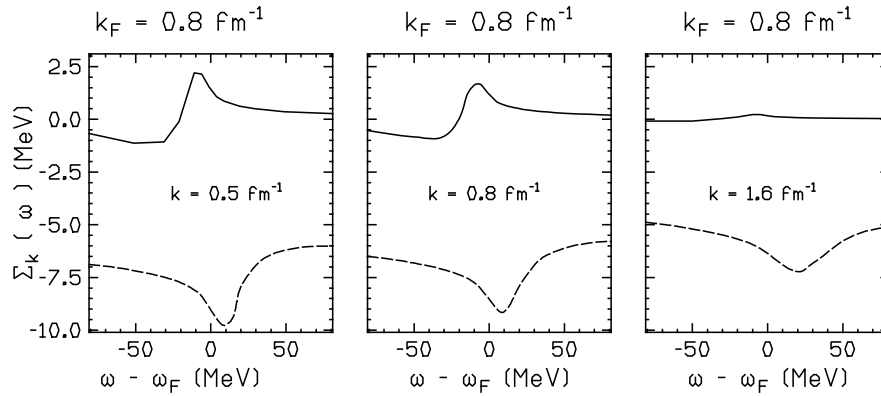


**Fig. 10.** Off-shell self-energy in neutron matter at  $k_F = 0.8 \text{ fm}^{-1}$ . *Solid curves:* BHF approximation  $\Sigma^{(1)}$ . *Dashed curves:* rearrangement contribution  $\Sigma^{(2)}$ . The Argonne  $V_{14}$  potential [24] has been used in the Brueckner calculations

In this case the quasiparticle energy takes the simple form

$$\omega_k \approx \frac{k^2 - k_F^2}{2m} \frac{1 + (m/k_F)(\partial\Sigma/\partial k)|_F}{1 - (\partial\Sigma/\partial\omega)|_F} = \frac{k^2 - k_F^2}{2m^*}. \quad (53)$$

In the previous equation we have introduced the effective mass  $m^*/m$  as the product of the  $e$ -mass  $m_e$  and the  $k$ -mass  $m_k$ , which are defined respectively as follows [75]

$$\frac{m_e}{m} = 1 - \frac{\partial\Sigma}{\partial\omega}\Big|_F = \frac{1}{Z_F}, \quad (54a)$$

$$\frac{m_k}{m} = \left[ 1 + \frac{m}{k_F} \frac{\partial\Sigma}{\partial k}\Big|_F \right]^{-1}. \quad (54b)$$

The partial derivatives are evaluated at the Fermi surface. The  $k$ -mass is related to the non-locality of the mean field and, in the static limit ( $\omega = \omega_F$ ), coincides with the effective mass. This quantity is of great interest in heavy-ion collision physics, since the transverse flows are very sensitive to the momentum dependence of the mean field. The  $e$ -mass is related to the quasi-particle strength. This latter gives the discontinuity of the neutron momentum distribution at the Fermi surface, and measures the amount of correlations included in the adopted approximation.

From  $\Sigma_k(\omega)$  the effective masses are extracted according to Eqs. (54a) and (54b). They are depicted in Fig. 11, where the full calculation is compared to

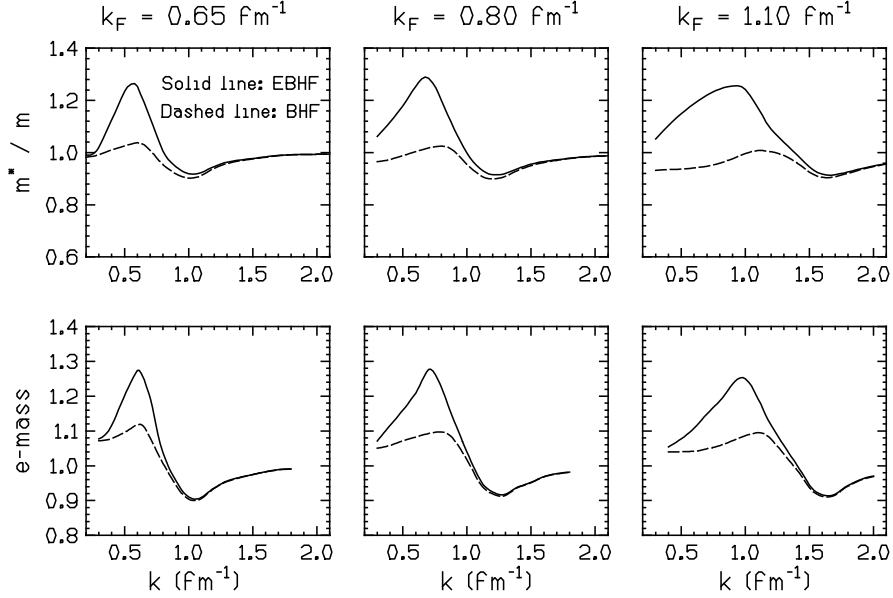


**Fig. 11.** Effective masses in neutron matter for three densities: effective mass  $m^*$  (upper panels) and  $e$ -mass (lower panels). Dashed lines correspond to  $\Sigma^{(1)}$  and solid lines to  $\Sigma^{(1)} + \Sigma^{(2)}$

that including only the BHF self-energy. We may distinguish two momentum intervals: at  $k \approx k_F$  the momentum dependence of the effective mass  $m^*$  is characterized by a bump, whose peak value exceeds the value of the bare mass; far above  $k_F$  the bare mass limit is approached. The contribution from the rearrangement term exhibits a pronounced enhancement in the vicinity of the Fermi energy, which is to be traced back to the high probability amplitude for p-h excitations near  $\epsilon_F$  [76]. At high momenta this contribution vanishes. One should take into account that in this range of  $k_F$  the neutron density is quite small ( $\rho = 0.074 \text{ fm}^{-3}$  at the maximum  $k_F = 1.3 \text{ fm}^{-1}$ ). This behaviour of the effective mass  $m^*$  is mostly due to the  $e$ -mass, as shown in the lower panels of Fig. 11. In all panels of Fig. 11 is also reported for comparison the effective mass in the BHF limit (only  $\Sigma^{(1)}$  included), which exhibits a much less pronounced bump at the Fermi energy.

With the off-shell values of the self-energy discussed above as input, the gap equation has been solved in the form of Eq. (48), coupled with Eq. (50) [77]. This is a quite satisfactory approximation, especially in view of studying the self-energy effects on pairing. The Argonne  $V_{14}$  potential has been adopted as pairing interaction, which is consistent with the self-energy data for which the same force has been used. The results are reported in Fig. 12 for a set of different  $k_F$ -values. The diamonds connected by a solid line represent the solution of Eq. (48) replacing the effective mass by the free one,  $m^* = m$ , together with  $Z = 1$ . This is very close to the prediction obtained from the BHF approximation

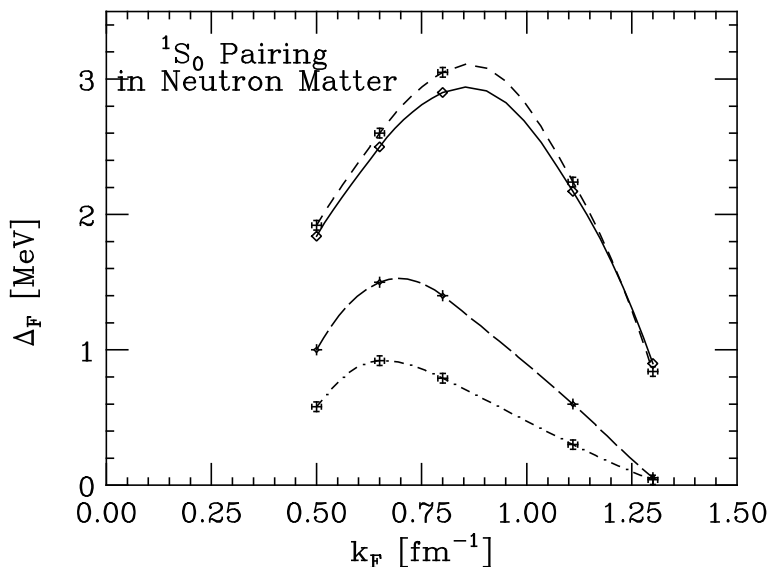


**Fig. 12.** Energy gap in different approximations for the self-energy: free s.p. spectrum (solid line); effective mass with  $Z_F = 1$  (upper dashed line);  $Z$  from  $\Sigma^{(1)}$  (long dashed line);  $Z$  from  $\Sigma^{(1)} + \Sigma^{(2)}$  (lower dashed line)

for the effective mass  $m^*$ , but still keeping  $Z = 1$  (fancy crosses connected by the dashed line). This similarity stems from the fact that at the Fermi surface  $m^*/m$  from BHF is close to one, as shown in Fig. 11. The self-energy effects are estimated in two approximations. In the first one  $m^*$  and the  $Z$ -factor are calculated from a BHF code. In the considered density domain the  $Z$ -factor ranges around 0.9. Despite its moderate reduction a dramatic suppression of the gap is obtained, as shown by the long dashed line in Fig. 12. It is due to the exponential dependence of the gap on all quantities. Still a further but more moderate reduction is obtained when the rearrangement term is included in the second approximation. The smaller  $Z$ -factor ( $Z \approx 0.83$  at  $k_F = 0.8 \text{ fm}^{-1}$ ) is to a certain extent counterbalanced by an increase of the effective mass ( $m^*/m \approx 1.2$  at the same  $k_F$ ).

From the previous discussion we may conclude that including self-energy effects is an important step forward in understanding the pairing in nucleon matter, but one should also include, on an equal footing, vertex corrections.

## 4 Conclusions

This chapter addressed the present status of the theoretical progress on the superfluidity of neutron matter and the microscopic calculations of nucleonic pairing gaps relevant for the conditions that are encountered in the interior of a neutron star. We have seen that most of the results that can be found in the literature, are obtained within the BCS approximation.

Unfortunately, as has also been pointed out, this approximation cannot be considered reliable in any region of density, since neutron matter is a strongly correlated Fermi system: The same nucleons that participate to the pairing coupling also participate to screen the pairs. This requires necessarily to improve the interaction kernel by in-medium polarization corrections that, at the present time, can be treated with confidence only at very low density, where the ring series can be truncated at the order of the one-bubble term.

The induced interaction approach is a promising candidate to describe these effects, but its predictions are still affected by too severe approximations. The existing calculations addressing this problem point to a substantial reduction of pairing in the ( $T = 1$ )  $^1S_0$  channel with respect to the BCS results. In the  $^3PF_2$  channel, no estimate of polarization effects has been made so far, at all.

Also self-energy effects, when properly included in the gap equation, strongly influence the pairing mechanism. We saw in fact that the gap is reduced with the square of the quasi-particle strength  $Z$ .

In any case it remains the problem of a complete solution of the generalized gap equation, taking into account simultaneously screening and self-energy corrections, which moreover have to be treated on the same footing. This latter goal remains a considerable theoretical challenge for the future.

Due to lack of space and time we have not discussed more speculative subjects like pairing in isospin asymmetric matter, relativistic effects on pairing, hyperon pairing, etc., which might also have relevance for neutron star physics.

## References

1. A. B. Migdal, Soviet Physics JETP **10**, 176 (1960).
2. J. A. Sauls, in *Timing Neutron Stars*, ed. by H. Ögelman and E. P. J. van den Heuvel, (Dordrecht, Kluwer, 1989) pp. 457.
3. *The Structure and Evolution of Neutron Stars*, Proc. US-Japan Joint Seminar, Kyoto, 6-10 November 1990, ed. by D. Pines, R. Tamagaki, and S. Tsuruta, (Addison-Wesley, Reading, 1992).
4. S. Tsuruta, Phys. Rep. **292**, 1 (1998).
5. H. Heiselberg and M. Hjorth-Jensen, Phys. Rep. **328**, 237 (2000).
6. J. Bardeen, L. N. Cooper, and J. R. Schrieffer, Phys. Rev. **108**, 1175 (1957).
7. A. Bohr, B. Mottelson, and D. Pines, Phys. Rev. **110**, 936 (1958).
8. A. Bohr, B. Mottelson, *Nuclear Structure*, Vol. 2 (Benjamin, New York, 1974).
9. L. N. Cooper, R. L. Mills, and A. M. Sessler, Phys. Rev. **114**, 1377 (1959).
10. V. J. Emery and A. M. Sessler, Phys. Rev. **119**, 248 (1960).
11. R. Tamagaki, Prog. Theor. Phys. **44**, 905 (1970).
12. T. Takatsuka and R. Tamagaki, Prog. Theor. Phys. Suppl. **112**, 27 (1993).
13. J. M. C. Chen, J. W. Clark, R. D. Davé, and V. V. Khodel, Nucl. Phys. **A555**, 59 (1993).
14. U. Lombardo, ‘Superfluidity in Nuclear Matter’, in *Nuclear Methods and Nuclear Equation of State*, ed. by M. Baldo, (World Scientific, Singapore, 1999) pp. 458-510.
15. A. A. Abrikosov, L. P. Gorkov, and I. E. Dzyaloshinskii, *Methods of Quantum Field Theory in Statistical Physics* (Prentice-Hall, Englewood Cliffs, 1963).
16. P. Nozières, *Le problème à N corps* (Dunod, Paris, 1963).
17. P. Nozières, *Theory of Interacting Fermi Systems* (Benjamin, New York, 1966).
18. J. R. Schrieffer, *Theory of Superconductivity* (Addison-Wesley, New York, 1964).
19. A. B. Migdal, *Theory of Finite Systems and Applications to Atomic Nuclei* (Benjamin, New York, 1964).
20. P. Ring and P. Schuck, *The Nuclear Many-Body Problem* (Springer, Berlin, 1980).
21. M. Baldo, I. Bombaci, and U. Lombardo, Phys. Lett. **B283**, 8 (1992).
22. M. Baldo, U. Lombardo, and P. Schuck, Phys. Rev. **C52**, 975 (1995).
23. M. Lacombe, B. Loiseaux, J. M. Richard, R. Vinh Mau, J. Côté, D. Pirès, and R. de Tournel, Phys. Rev. **C21**, 861 (1980).
24. R. B. Wiringa, R. A. Smith, and T. L. Ainsworth, Phys. Rev. **C29**, 1207 (1984).
25. R. Machleidt, Adv. Nucl. Phys. **19**, 189 (1989).
26. V. G. J. Stoks, R. A. M. Klomp, C. P. F. Terheggen, and J. J. de Swart, Phys. Rev. **C48**, 792 (1993).
27. R. B. Wiringa, V. G. J. Stoks, and R. Schiavilla, Phys. Rev. **C51**, 38 (1995).
28. R. Machleidt, F. Sammarruca, and Y. Song, Phys. Rev. **C53**, 1483 (1996).
29. L. Amundsen and E. Østgaard, Nucl. Phys. **A442**, 163 (1985).
30. M. Baldo, J. Cugnon, A. Lejeune, and U. Lombardo, Nucl. Phys. **A536**, 349 (1992).
31. Ø. Elgarøy, L. Engvik, M. Hjorth-Jensen, and E. Osnes, Nucl. Phys. **A607**, 425 (1996).
32. M. Baldo, Ø. Elgarøy, L. Engvik, M. Hjorth-Jensen, and H.-J. Schulze, Phys. Rev. **C58**, 1921 (1998).
33. V. A. Khodel, V. V. Khodel, and J. W. Clark, Phys. Rev. Lett. **81**, 3828 (1998).
34. A. L. Goodman, Nucl. Phys. **A186**, 475 (1972); Phys. Rev. **C60**, 014331 (1999).
35. L. Amundsen and E. Østgaard, Nucl. Phys. **A437**, 487 (1985).
36. M. Baldo, J. Cugnon, A. Lejeune, and U. Lombardo, Nucl. Phys. **A515**, 409 (1990).
37. V. A. Khodel, V. V. Khodel, and J. W. Clark, Nucl. Phys. **A598**, 390 (1996).

38. Ø. Elgarøy and M. Hjorth-Jensen, *Phys. Rev.* **C57**, 1174 (1998).
39. T. Alm, G. Röpke, and M. Schmidt, *Z. Phys.* **A337**, 355 (1990).
40. B. E. Vonderfecht, C. C. Gearhart, W. H. Dickhoff, A. Polls, and A. Ramos, *Phys. Lett.* **B253**, 1 (1991).
41. T. Alm, B. L. Friman, G. Röpke, and H. Schulz, *Nucl. Phys.* **A551**, 45 (1993).
42. H. Stein, A. Schnell, T. Alm, and G. Röpke, *Z. Phys.* **A351**, 295 (1995).
43. T. Alm, G. Röpke, A. Sedrakian, and F. Weber, *Nucl. Phys.* **A406**, 491 (1996).
44. M. Baldo, U. Lombardo, P. Schuck, and A. Sedrakian, *Condensed Matter Theories*, Vol. 12, ed. by J. W. Clark (Nova Science Publishers, 1997), pp. 265-277.
45. Ø. Elgarøy, L. Engvik, E. Osnes, and M. Hjorth-Jensen, *Phys. Rev.* **C57**, R1069 (1998).
46. U. Lombardo, H.-J. Schulze, and W. Zuo, *Phys. Rev.* **C59**, 2927 (1999).
47. A. Sedrakian, G. Röpke, and T. Alm, *Nucl. Phys.* **A594**, 355 (1995).
48. A. Sedrakian, T. Alm, and U. Lombardo, *Phys. Rev.* **C55**, R582 (1997).
49. G. Röpke, A. Schnell, P. Schuck, and U. Lombardo, *Phys. Rev.* **C61**, 024306 (2000).
50. A. Sedrakian and U. Lombardo, *Phys. Rev. Lett.* **84**, 602 (2000).
51. J. Cugnon, P. Deneye, and A. Lejeune, *Z. Phys.* **A326**, 409 (1987).
52. I. Bombaci and U. Lombardo, *Phys. Rev.* **C44**, 1892 (1991).
53. W. Zuo, I. Bombaci, and U. Lombardo, *Phys. Rev.* **C60**, 024605 (1999).
54. Ø. Elgarøy, L. Engvik, M. Hjorth-Jensen, and E. Osnes, *Nucl. Phys.* **A604**, 466 (1996).
55. M. Baldo, G. F. Burgio, and H.-J. Schulze, *Phys. Rev.* **C58**, 3688 (1998); **C61**, 055801 (2000).
56. I. Vidaña, A. Polls, A. Ramos, L. Engvik, and M. Hjorth-Jensen, *Phys. Rev.* **C62**, 035801 (2000).
57. P. W. Anderson and P. Morel, *Phys. Rev.* **123**, 1911 (1961).
58. A. L. Fetter and J. D. Walecka, *Quantum Theory of Many-Particle Systems* (McGraw-Hill, New-York, 1971).
59. L. P. Gorkov and T. K. Melik-Barkhudarov, *Sov. Phys. JETP* **13**, 1018 (1961).
60. T. Papenbrock and G. F. Bertsch, *Phys. Rev.* **C59**, 2052 (1999).
61. H. Heiselberg, C. J. Pethick, H. Smith, and L. Viverit, *Phys. Rev. Lett.* **85**, 2418 (2000).
62. J. W. Clark, C.-G. Källman, C.-H. Yang, and D. A. Chakkalakal, *Phys. Lett.* **B61**, 331 (1976).
63. J. M. C. Chen, J. W. Clark, E. Krotschek, and R. A. Smith, *Nucl. Phys.* **A451**, 509 (1986).
64. T. L. Ainsworth, J. Wambach, and D. Pines, *Phys. Lett.* **B222**, 173 (1989).
65. J. Wambach, T. L. Ainsworth, and D. Pines, *Nucl. Phys.* **A555**, 128 (1993).
66. H.-J. Schulze, J. Cugnon, A. Lejeune, M. Baldo, and U. Lombardo, *Phys. Lett.* **B375**, 1 (1996).
67. S. Babu and G. E. Brown, *Ann. Phys. (N.Y.)* **78**, 1 (1973).
68. O. Sjöberg, *Ann. Phys. (N.Y.)* **78**, 39 (1973).
69. S.-O. Bäckmann, C.-G. Källman, and O. Sjöberg, *Phys. Lett.* **43B**, 263 (1973).
70. A. D. Jackson, E. Krotschek, D. E. Meltzer, and R. A. Smith, *Nucl. Phys.* **A386**, 125 (1982).
71. W. H. Dickhoff, A. Faessler, H. Mütter, and Shi-Shu Wu, *Nucl. Phys.* **A405**, 534 (1983).
72. S.-O. Bäckmann, G. E. Brown, and J. A. Niskanen, *Phys. Rep.* **124**, 1 (1985).
73. P. Bozek, *Nucl. Phys.* **A657**, 187 (1999); *Phys. Rev.* **C62**, 054316 (2000).
74. M. Baldo and A. Grasso, *Phys. Lett.* **B485**, 115 (2000).

- 75. J. P. Jeukenne, A. Lejeune, and C. Mahaux, Phys. Rep. **25C**, 83 (1976).
- 76. Zuo Wei, G. Giansiracusa, U. Lombardo, N. Sandulescu, and H.-J. Schulze, Phys. Lett. **B421**, 1 (1998).
- 77. U. Lombardo and P. Schuck, 'Self-energy effects in neutron matter superfluidity', to be published.